ISSN 1070-3284, Russian Journal of Coordination Chemistry, 2017, Vol. 43, No. 11, pp. 795–799. © Pleiades Publishing, Ltd., 2017.

Divanadate-Based Inorganic-Organic Hybrid Compound: $\{[Cu(En)_2]_2V_2O_7\} \cdot 4H_2O$[1]

K. Wang[a, b], J. Li[a], Z. J. Liang[a], P. T. Ma[a], D. D. Zhang[a], J. Y. Niu[a, *], and J. P. Wang[a, **]

[a] *Henan Key Laboratory of Polyoxometalate Chemistry, College of Chemistry and Chemical Engineering, Henan University, Kaifeng, 475004 P.R. China*

[b] *Department of Pharmacy, Henan Medical College, Zhengzhou, 451191 P.R. China*

**e-mail: niujy@henu.edu.cn*

***e-mail: jpwang@henu.edu.cn*

Received December 15, 2016

Abstract—A new compound $\{[Cu(En)_2]_2V_2O_7\} \cdot 4H_2O$ (**I**) (En = ethanediamine) has been synthesized by the combination of hydrothermal and solvent evaporation method and characterized by single-crystal X-ray diffraction (CIF file CCDC no. 1450218), IR, UV-Vis spectra, thermogravimetric analysis, powder X-ray diffraction, and fluorescence analysis. Crystal data for **I**: $C_8H_{40}Cu_2N_8O_{11}V_2$, $Mr = 653.44$, orthorhombic, space group *Cmca*, $a = 18.559(11)$, $b = 17.583(11)$, $c = 7.600(6)$ Å, $V = 2480(3)$ Å^3, and $Z = 4$. Interestingly, two $[Cu(En)_2]^{2+}$ coordination cations are bridged by the $[V_2O_7]^{4-}$ unit to build up a neutral framework compound.

Keywords: crystal structure, divanadate, fluorescence emission, metal organoamine

DOI: 10.1134/S1070328417110112

INTRODUCTION

The inorganic-organic hybrid materials have been developed enormously owing to their potential applications in the fields of medicine, catalysis, liquid crystals, proton conductivity, and photochemistry [1–7]. The important feature of these hybrid assemblies is combination of the merit from inorganic and organic building blocks, which endows them with new structures and composite properties [8, 9]. Polyoxometalates with definite sizes and shapes are unmatched inorganic components. Polyoxovanadates (POVs), as an important subclass of polyoxometalates, can form a large variety of high- or low-nuclearity cluster structures, due to the various coordination geometries of vanadium ion (including VO_4 tetrahedra, VO_5 square pyramid, and VO_6 octahedra), therefore becoming one of the best candidates for the inorganic component of such hybrid materials [10]. In this field, divanadate, as the simplest polyoxovanadate, exists in the form of $[V_2O_5]^-$, $[V_2O_6]^{2-}$ and $[V_2O_7]^{4-}$. Amongst them, $[V_2O_5]^-$ and $[V_2O_6]^{2-}$ can be linked into two-dimensional vanadium oxide layers and one-dimensional vanadium oxide chains through interlinking $\{VO_5\}$ and $\{VO_4\}$ polyhedrons, respectively, or further linked into three-dimensional structure via metal-organoamine complexes [11–13]. In the past 15 years, several compounds based on $[V_2O_7]^{4-}$ such as $M_2V_2O_7$ (with M = Mg, Ca, Zn, Cd, Ba, and Cu) [14, 15], $(CsCl)Mn_2(V_2O_7)$ [16], and $AgFeV_2O_7$ [17] have been synthesized by high temperature solid-phase reaction method, which were mainly used as the cathode material of lithium-ion batteries. In addition, the other $\{V_2O_7\}$-based compound $[Cu_2F_2(C_{10}H_{10}N_3)_2][V_2O_7]$ [18] was obtained under hydrothermal condition. Although divanadates have been investigated intensively, however, to our knowledge, $\{V_2O_7\}$-containing inorganic-organic hybrid materials have not been reported except the compound $[Cu_2F_2(C_{10}H_{10}N_3)_2][V_2O_7]$ [18]. Herein, we launch the exploration of inorganic-organic hybrid polyoxovanadate and present the synthesis and structure characterization of divanadate compound $\{[Cu(En)_2]_2V_2O_7\} \cdot 4H_2O$ (**I**). It represents a new example of the divanadate $[V_2O_7]^{4-}$ cluster modified by copper complexes $[Cu(En)_2]^{2+}$.

EXPERIMENTAL

Methods and instruments. All reagents were used as purchased without further purification. Elemental analyses (C, H, and N) were performed by a Perkin-Elmer 2400-II CHNS/O analyzer. IR spectrum was recorded on a Bruker VERTEX 70 IR spectrometer using KBr as pellets in the range of 4000–450 cm^{-1} region. UV absorption spectrum was obtained with a

[1] The article is published in the original.

Table 1. Selected bond lengths (Å) and bond angles (deg) for **I***

Bond	*d*, Å	Bond	*d*, Å	Bond	*d*, Å
V(1)–O(1)	1.7889(17)	V(1)–O(4)	1.669(6)	Cu(1)–N(2)	2.001(6)
V(1)–O(2)	1.690(5)	Cu(1)–N(1)	2.029(6)	Cu(1)–O(4)	2.210(6)
Angle	ω, deg	Angle	ω, deg	Angle	ω, deg
O(2)V(1)O(1)	110.81(18)	O(4)V(1)O(2)	109.3(2)	NCu(1)N	84.9(3)
O(2)^{1}V(1)O(2)	109.3(4)	V(1)O(4)Cu(1)	127.3(4)	NCu(1)O	92.8(2)
O(4)V(1)O(1)	107.3(2)				

* Symmetry transformation: ^{1} $-x, y, z$.

U-4100 spectrometer in 200–400 nm at room temperature. Thermogravimetric (TG) analysis was carried out under N_2 flow with a Mettler-Toledo TGA/SDTA 851 instrument at a heating rate of 10°C/min from 25 up to 500°C. Powder X-ray diffraction (PXRD) was performed on a Bruker AXS D8 Advance diffractometer using CuK_α radiation (λ = 1.54056 Å) in the range 2θ = 5°–45° at 293 K. Fluorescence spectrum was performed on a HITACHI F-7000 fluorescence spectrophotometer with a Xe lamp as the light source at room temperature.

Synthesis of I. NH_4VO_3 (0.25 g, 2.14 mmol), $CuCl_2 \cdot 2H_2O$ (0.15 g, 0.88 mmol) and Sb_2O_3 (0.23 g, 0.79 mmol) were stirred in a mixed solution of 4 mL distilled water and 4 mL En for 10 min, forming a brown suspension solution. The pH was adjusted to 13.0 with 2 mol/L NaOH solution. The resulting solution was sealed in 25 mL Teflon lined stainless steel autoclave and heated at 130°C for 6 days, then cooled to room temperature. The clear violet filtrate was kept in an open beaker at room temperature to allow slow evaporation. Subsequent crystallization about one week yielded a blue block with the yield of 15% (based on vanadium).

IR (ν, cm^{-1}): 3369, 3309, 3218, 3139, 2965, 2194, 2886, 1583, 1452, 1384, 1319, 1164, 1106, 1044, 975, 921, 840, 673, 525, 404.

For $C_8H_{40}N_8O_{11}V_2Cu_2$

Anal. calcd., %:	C, 14.70;	H, 6.17;	N, 17.15.
Found, % :	C, 14.91;	H, 6.44;	N, 17.48.

X-ray crystal determination. Single crystal X-ray diffraction data collections for **I** were performed on a Bruker APEX-II CCD diffractometer with graphite monochromated MoK_α radiation (λ = 0.71073 Å) at 293(2) K. All of the absorption corrections were performed with the SADABS program. The structures were solved by direct methods and non-hydrogen atoms were refined by full-matrix least-squares methods on F^2 using the SHELX program suite [19]. The hydrogen atoms of the organoamine groups were placed in calculated positions and then refined using a riding model with a uniform value of $U_{iso} = 1.2\ U_{eq}$. All H atoms on water molecules were directly included in the molecular formula. Crystal data and structure refinement for **I**: $C_8H_{40}Cu_2N_8O_{11}V_2$, Mr = 653.44; blue block crystal, 0.28 × 0.16 × 0.08 mm; T = 293(2) K; orthorhombic, space group *Cmca*; a = 18.559(11), b = 17.583(11), c = 7.600(6) Å; V = 2480(3) Å^3; Z = 4; μ = 2.482 mm^{-1}; $F(000)$ = 1312.0; 5848 reflections measured, of which 1141 were independent; R_1 = 0.0853, and wR_2 = 0.2181; ρ_{calcd} = 1.728 g/cm^3.

The selected bond lengths and band angles are shown in Table 1. Supplementary crystallographic data for the structure of **I** has been deposited with the Cambridge Crystallographic Data Centre (CCDC no. 1450218; deposit@ccdc.cam.ac.uk or http://www.ccdc.cam.ac.uk).

RESULTS AND DISCUSSION

Single crystal X-ray diffraction analysis reveals that compound **I** is composed of two $[Cu(En)_2]^{2+}$ coordination cations, one $[V_2O_7]^{4-}$ polyanion, and four lattice water molecules. Interestingly, the $\{V_2O_7\}$ unit can be seen as two $\{VO_4\}$ tetrahedron via sharing a corner, in which three μ_2-O atoms and two vanadium atoms connect together forming a folded-line-shaped skeleton (Fig. 1). This kind of connection mode is quite unusual in the divanadate. In addition, the two copper ions are five-coordinated square pyramid configuration with four nitrogen atoms from two En molecules and an oxygen atom from $\{V_2O_7\}$ group residing both sides of $\{V_2O_7\}$ fragment, thus they function as counterions decorating the whole cluster (Fig. 1). Within all four oxygen atoms, the O(2), O(3) atoms are terminal type and the other oxygen atoms O(4) and O(1) are μ_2-O type. Band-valence sum (BVS) calculation values for V atoms and Cu atoms are +5 and +2, respectively, which indicates vanadium atoms are in fully oxidized state. The anion of **I** has the same $[V_2O_7]^{4-}$ core reported previously for $[AgFeV_2O_7]$ and $[(CsCl)Mn_2(V_2O_7)]$. However, in $[AgFeV_2O_7]$, four of the six terminal oxygens of the $\{V_2O_7\}$ unit are shared

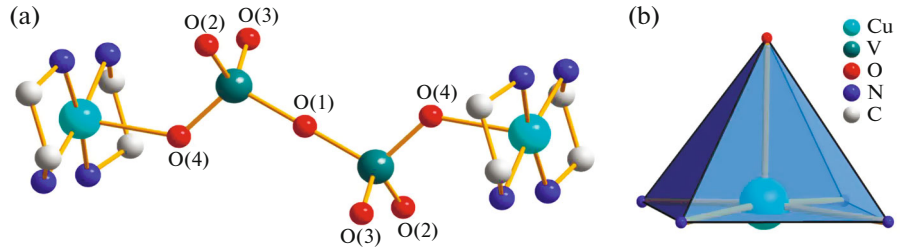

Fig. 1. The ball and stick view of the neutral cluster $\{[Cu(En)_2]_2V_2O_7\}$ (a); the polyhedron graphics of the coordination cation $[Cu(En)_2]^{2+}$ (b). H atoms are omitted for clarity.

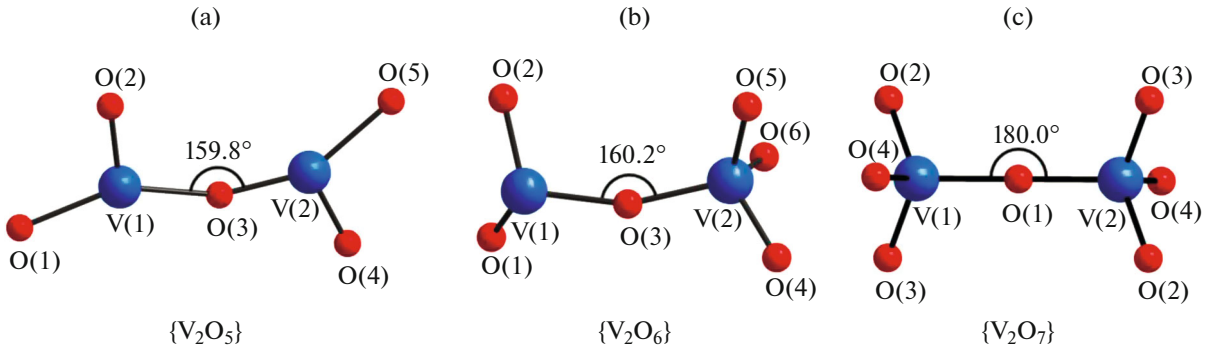

Fig. 2. The ball and stick view of the different $\{V_2\}$ units and their VOV angles: $\{V_2O_5\}$ unit [8] (a); $\{V_2O_6\}$ unit [9] (b); $\{V_2O_7\}$ unit in our works (c).

with four Fe_2O_{10} octahedron dimers along [100], and the fifth oxygen is shared with another dimer to extend the lattice along the (011) plane, leading to the formation of three-dimensional structure [17]. In $[(CsCl)Mn_2(V_2O_7)]$ [16], six terminal O atoms of the $\{V_2O_7\}$ cluster bind to eight MnO_4Cl_2 octahedron, forming a three-dimensional network.

It should be noted that the $[V_2O_7]^{4-}$ group with D_{3d} symmetry is different from the other two $[V_2O_5]^-$ [11] and $[V_2O_6]^{2-}$ [12] asymmetric units. As shown in Fig. 2, the bond angle of VOV is 159.8°, 160.2°, 180° in $\{V_2O_5\}$, $\{V_2O_6\}$ and $\{V_2O_7\}$, respectively. Additionally, from the viewpoint of copper complex ion, the Cu^{2+} ion in $[Cu(En)_2H_2O]^{2+}$ fragment of $[Cu(En)_2(H_2O)]_2[H_2V_{10}O_{28}] \cdot 12H_2O$ [20] is six coordinated by four nitrogen atoms from two en molecules (Cu(1)–N(1) 2.009 Å, Cu(1)–N(2) 2.012 Å, Cu(1)–N(3) 2.001 Å, Cu(1)–N(4) 2.004 Å), two oxygen atoms from the $[H_2V_{10}O_{28}]^{4-}$ anion (Cu(1)–O(8) 2.530 Å) and one water molecule (Cu(1)–O(15) 2.668 Å). In contrast, the Cu–O bond length in $[Cu(En)_2]^{2+}$ fragments of **I** (Table 1) is obviously less than those of $[Cu(En)_2(H_2O)]^{2+}$. This may be attributed to the difference of coordination configuration of the two fragments.

The thermogravimetric analysis (TG) of **I** is performed in the temperature range of 25–500°C in nitrogen gas. The total weight loss value of 48.60% (calcd. 47.82%) between 25 and 500°C are attributed to the removal of the four lattice water molecules and four ethanediamine molecules. The first weight loss of 11.77% (calcd. 11.03%) corresponding to the four lattice water molecules is in the region of 25–175°C. The last mass loss in the regions of 175–500°C can be assigned to the sublimation of four ethanediamine molecules (exptl 36.83%, calcd. 36.79%). The TG curve of compound **I** is shown in Fig. 3.

The IR spectrum of **I** is shown in Fig. 3. The characteristic symmetric stretch vibration $\nu(V{=}O_{terminal})$ is located at 921 cm^{-1} and a number of bands in the range 840 to 525 cm^{-1} are associated with $\nu_{as}(V–O_b–V)$. The band at 3369 cm^{-1} can be attributed to O–H stretching of lattice water molecules. Additionally, the stretching bands of NH_2 and CH_2 groups are observed at ν = 3139 to 3309 cm^{-1} and 2886 to 2965 cm^{-1}, respectively, and their bending bands at ν = 1583 to 1452 cm^{-1} and 1318 to 1384 cm^{-1}, respectively, which confirm the presence of En in **I**. The assignment of the vibration modes is in accordance with the published results [20–23]. In addition, the peak positions of the simulated and experimental PXRD patterns match well with each other (Fig. 3), which indicates the phase purity of the title compound.

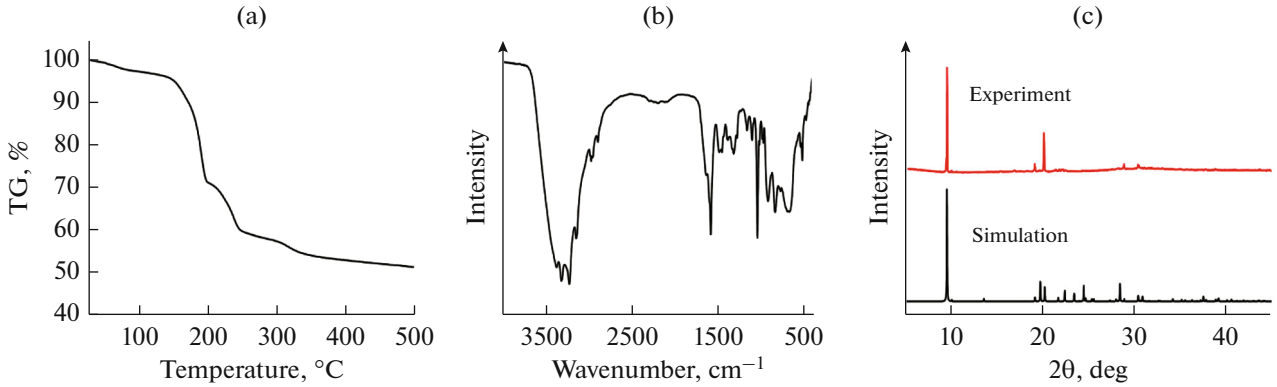

Fig. 3. The TG curve of **I** (a); the IR spectrum of **I** (b); the experiment and simulation PXRD patterns of **I** (c).

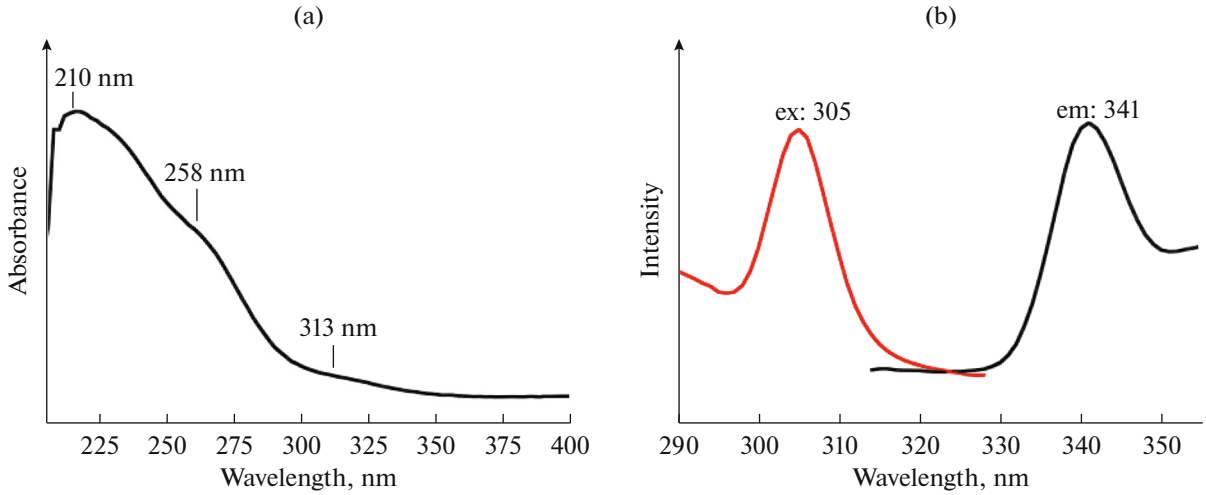

Fig. 4. The UV spectrum of **I** (a); the fluorescence spectrum of **I** at room temperature in aqueous solution (b).

The UV-Vis spectrum of **I** in aqueous solution displays three absorption peaks at 210, 258 nm (sh) and 313 nm (Fig. 4), corresponding to oxide-to-vanadium charge transfer (LMCT) [7, 24–26]. The fluorescent spectrum of **I** at room temperature in aqueous solution is depicted in Fig. 4. The compound **I** shows one peak at 341 nm upon excitation at 305 nm corresponding to oxide-to-vanadium charge transfer (O^{2-} to V^{5+}) which is comparable with the UV absorption spectrum. It can be considered that the emissive state of **I** is likely derived from the O^{2-} to V^{5+} charge transfer as the literature reported by Hong [7].

Thus, a new cluster compound $\{[Cu(En)_2]_2V_2O_7\} \cdot 4H_2O$ has been synthesized by the combination of hydrothermal and solvent evaporation method. The binuclear $[V_2O_7]^{4-}$ vanadate decorated by transition metal complex $[Cu(En)_2]^{2+}$ cations features a discrete neutral-framework structure. In addition, the fluorescent properties of the compound **I** were investigated in detail, electron transition transferred from O^{2-} to V^{5+} produce the fluorescence-emission of 341 nm.

ACKNOWLEDGMENTS

This work was supported by the Natural Science Foundation of China (grant no. 21573056).

REFERENCES

1. Haag, R., *Angew. Chem. Int. Ed.*, 2004, vol. 43, p. 278.
2. Griset, A.P., Walpole, J., Liu, R., et al., *J. Am. Chem. Soc.*, 2009, vol. 131, p. 2469.
3. Kanie, K. and Sugimoto, T., *J. Am. Chem. Soc.*, 2003, vol. 125, p. 10518.
4. Hoffmann, F., Cornelius, M., Morell, J., and Fröba, M., *Angew. Chem. Int. Ed.*, 2006, vol. 45, p. 3216.
5. Proust, A., Thouveno, R., and Gouzerh, P., *Chem. Commun.*, 2008, p. 1837.

6. Wei, M.L., Sun, J.J., and Duan, X.Y., *Eur. J. Inorg. Chem.*, 2014, p. 345.
7. Chen, L., Jiang, F.L., Lin, Z.Z., et al., *J. Am. Chem. Soc.*, 2005, vol. 127, p. 8588.
8. Cariati, E., Macchi, R., Roberto, D., et al., *J. Am. Chem. Soc.*, 2007, vol. 129, p. 9410.
9. Corma, A., Díaz, U., García, T., et al., *J. Am. Chem. Soc.*, 2010, vol. 132, p. 15011.
10. Breen, J.M. and Schmitt, W., *Angew. Chem. Int. Ed.*, 2008, vol. 47, p. 6904.
11. Shan, Y.K., Huang, R.H., and Huang, S.D., *Angew. Chem. Int. Ed.*, 1999, vol. 38, p. 1751.
12. Khan, M.I., Yohannes, E., Golub, V.O., et al., *Chem. Mater.*, 2007, vol. 19, p. 4890.
13. Khan, M.I., Yohannes, E., Nome, R.C., et al., *Chem. Mater.*, 2004, vol. 16, p. 5273.
14. Nielsen, U.G., Jakobsen, H.J., and Skibsted, J., *J. Phys. Chem., B.*, 2001, vol. 105, p. 420.
15. Calvo, C. and Faggiani, R., *Acta. Crystallogr., Sect. B: Struct. Sci.*, 1975, vol. 31, p. 603.
16. Queen, W.L., West, J.P., Hwu, S.-J., et al., *Angew. Chem. Int. Ed.*, 2008, vol. 47, p. 3791.
17. Becht, G.A., Vaughey, J.T., and Hwu, S.-J., *Chem. Mater.*, 2010, vol. 22, p. 1149.
18. Mahenthirarajah, T., Li, Y., and Lightfoot, P., *Inorg. Chem.*, 2008, vol. 47, p. 9097.
19. Sheldrick, G.M., *Acta. Crystallogr., Sect. A: Found. Crystallogr.*, 2008, vol. 64, p. 112.
20. Ma, H.Y., Meng, X., Sha, J.Q., et al., *Solid State Sci.*, 2011, vol. 13, p. 850.
21. Zheng, S.T., Zhang, J., Li, B., and Yang, G.Y., *Dalton Trans.*, 2008, p. 5584.
22. Antonova, E., Näther, C., and Bensch, W., *Dalton Trans.*, 2012, p. 1338.
23. Zhou, J., Zhang, J., Fang, W.H., and Yang, G.Y., *Chem. Eur. J.*, 2010, vol. 16, p. 13253.
24. Yamase, T., *Chem. Rev.*, 1998, vol. 98, p. 307.
25. Chen, Q., Goshorn, D.P., Scholes, C.P., et al., *J. Am. Chem. Soc.*, 1992, vol. 114, p. 4667.
26. Codd, R., Hambley, T.W., and Lay, P.A., *Inorg. Chem.*, 1995, vol. 34, p. 877.